ELSEVIER

Chemical Physics 236 (1998) 63–76

Chemical Physics

Electrical interaction between two spherical particles covered by an ion-penetrable charged membrane

Jyh-Ping Hsu *, Bo-Tau Liu

Department of Chemical Engineering, National Taiwan University, Taipei, 10617, Taiwan, ROC

Received 26 March 1998

Abstract

The electrical interaction between two spherical particles, each comprises a rigid uncharged core and an ion-penetrable (porous) charged membrane, in an electrolyte solution is examined. The Poisson equation governing the spatial variation of electrical potential is solved by the Green's function approach, and the interaction energy of the system under consideration evaluated. Several approximate analytical expressions for the interaction energy are derived. We show that if the membrane is thick, and/or the electrical double layer is either very thin or very thick, a particle can be treated as a porous one, and the linear superposition approach often adopted in the literature becomes appropriate. © 1998 Elsevier Science B.V. All rights reserved.

1. Introduction

The electrical potential distribution governed by the Poisson–Boltzmann equation plays a significant role in the description of the properties of a colloidal dispersion [1,2]. In the last two decades, the electrostatic interactions between two colloidal particles has been analyzed extensively. The relevant studies, however, are mainly focused on rigid particles, and relatively little attention is paid to ion-penetrable or porous particles, which simulate a wide class of colloidal particles in practice. Typical example includes biological cells, e.g., blood cells and protein aggregates [3–7], and entities covered by an artificial membrane, e.g., particles with an adsorbed polymer layer [8]. These particles are characterized by having an ion-penetrable surface, which usually bears fixed charge due to the dissociation of the functional groups it carries. For instance, the peripheral zone of human erythrocyte comprises a glycoprotein layer of ~ 15 nm thick which possesses some ionogenic groups, and forms the outer boundary of the lipid layer [9]. Ohshima et al. [10,11] analyzed the electrostatic interaction between two planar, ion-penetrable charged membranes. The analysis was also extended to spherical particles [12,13]; analytical expressions for the electrical potential and interaction energy between two particles were derived under the condition of low electrical potential. The problem of the interaction between two planar, charged membranes was also examined by Hsu et al. [14], taking the effect of the difference between the dielectric constant of the membrane phase and that of the liquid phase into account. Symmetric electrolytes and nonuniform fixed charge distribution were assumed in their study, and the governing equations were solved numerically. A numerical scheme was proposed by Hsu and Kuo [15] for the evaluation of the electrical

* Corresponding author. E-mail: t8504009@ccms.ntu.edu.tw

PII: S0301-0104(98)00197-9

potential between two planar, parallel membranes for the case of arbitrary electrolytes and nonuniform fixed charge distribution. The stability ratio and the critical coagulation concentration for spherical particles covered by an ion-penetrable membrane under low electrical potential were derived by Hsu and Kuo [16].

The reported results mentioned in the previous discussions are mainly based on the linear superposition, i.e., the result of two interacting entities is approximated by the sum of the results of two isolated entities through defining an appropriate global coordinate. While this approach simplifies the relevant analysis, it may lead to an appreciable deviation under the conditions of practical significance. Carnie et al. [17], for example, concluded that the deviation in the electrical interaction force between two identical, rigid spheres arises from the linear superposition is above 10% under the conditions that the ratios (closest distance between particles)/(Debye length) < 2 and (radius of particle)/(Debye length) = 2, and the scaled surface potential = 1. In the present study, an attempt is made to derive an exact expression for the electrical interaction energy between two spherical particles covered by a membrane layer. An approximate analytical expression for the interaction energy is also derived which is highly desirable in the discussion of the basic properties, such as the stability ratio and the critical coagulation concentration, of a colloidal dispersion.

2. Analysis

By referring to Fig. 1, we consider a system containing two spherical particles, each comprises a rigid, uncharged core and an ion-penetrable charged membrane, in an electrolyte solution. The particles may have different sizes. Let R be the distance between the centers of particles 1 and 2, a_i the radius of the rigid core of particle i $(i=1,2)$ and b_i the radius of particle i, r_{ij} the distance between the surface of particle i and the center of particle j. The membrane layer of a particle contains fixed charges, which may due to, for example, the dissociation of functional groups. Suppose that the electrical potential of the system under consideration is sufficiently low such that it can be described approximately by the linearized Poisson–Boltzmann equation

$$\Delta\psi = \kappa^2\psi, \quad \text{in solution}, \tag{1}$$

$$\Delta\psi = \kappa^2\psi - \rho_i/\varepsilon, \quad \text{inside membrane phase of particle } i, \tag{2}$$

with

$$\kappa^2 = 2F^2I/\varepsilon RT. \tag{2a}$$

In these expressions, ψ denotes the scaled electrical potential, Δ is the Laplace operator, ε is the dielectric constant, κ and ρ_i are, respectively, the reciprocal Debye length and the density of fixed charge inside the membrane phase of particle i, T is the absolute temperature, and F and I are the elementary charge and the ionic strength, respectively.

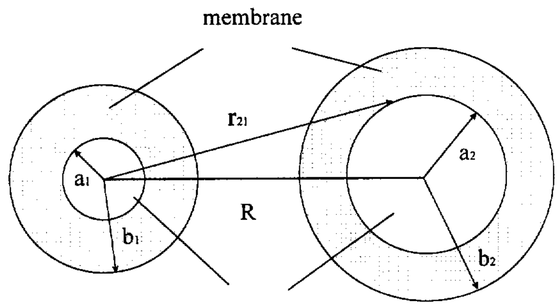

Fig. 1. Schematic representation of the system under consideration where R is the distance between the centers of particles 1 and 2, a_i the radius of the rigid core of particle i, b_i the radius of particle i, and r_{ij} the distance between the surface of particle i and the center of particle j.

It can be shown that a particular solution to Eq. (1) is [18]

$$G(r) = \frac{e^{-\kappa r}}{4\pi r}, \tag{3}$$

where r is the scaled distance from a fixed point charge (singular point), and G is known as the free Green's function. Combining Eqs. (1)–(3) and integrating over the entire domain excluding the rigid cores of the particles and the singular point, Ω, gives

$$\int_{\Omega} [\psi \Delta G - G \Delta \psi] \mathrm{d}\Omega = \frac{1}{\varepsilon} \sum_{i=1}^{2} \int_{V_i} \rho_i G \, \mathrm{d}V, \tag{4}$$

where V_i is the volume of the membrane phase of particle i. We assume that the dielectric constant of the rigid core of a particle is much smaller than that of the liquid phase, as is usually the case in practice. Suppose that the interface between the membrane layer and the rigid core of a particle is free of charges. This leads to the boundary condition

$$\left(\frac{\partial \psi}{\partial n_i} \right)_{S_i} = 0, \tag{5}$$

where S_i is the surface of the rigid core of particle i, and n_i the outward normal vector of S_i pointing to the bulk liquid phase. Applying Green's formula, the electrical potential can be obtained from Eqs. (4) and (5) as

$$\psi = \sum_{i=1}^{2} \left[\int_{S_i} \psi_{S_i} \chi_i \, \mathrm{d}S + \frac{1}{\varepsilon} \int_{V_i} \rho_i G \, \mathrm{d}V \right], \tag{6}$$

with

$$\chi_i = \frac{\partial G}{\partial n_i}. \tag{6a}$$

Similar to the potential theory [19], if the evaluated point is located on the surface of the rigid core of particle j, S_j, then

$$\frac{1}{2} \psi_{S_j} = \sum_{i=1}^{2} \left[\int_{S_i} \psi_{S_i} \chi_i \, \mathrm{d}S + \frac{1}{\varepsilon} \int_{V_i} \rho_i G \, \mathrm{d}V \right]. \tag{7}$$

The surface potential of the rigid core of particle i is determined by ρ_i. For illustration, we assume that ρ_i is constant, i.e., the fixed charges are uniformly distributed. It should be pointed out, however, that the present analysis does not limited to this type of fixed charge distribution.

Suppose that ψ_{S_i} can be decomposed as

$$\psi_{S_i} = \psi_{S_i}^0 + \Delta \psi_{S_i}, \tag{8}$$

where $\psi_{S_i}^0$ denotes the unperturbed surface potential of the rigid core of particle i, and $\Delta \psi_{S\mathrm{i}}$ represents a perturbed surface potential due to the presence of particle j. $\psi_{S_i}^0$ can be estimated by

$$\psi_{S_i}^0 = \frac{1}{\varepsilon} \frac{\beta_{ii}}{\frac{1}{2} - \gamma_{ii}}, \tag{9}$$

where β_{ii} and γ_{ii} are calculated at the points on the surface of the rigid core of particle i according to the expressions

$$\beta_{ii} = \int_{V_i} G \, \mathrm{d}V = \frac{\sinh(\kappa a_i)}{\kappa a_i} \left[\frac{e^{-\kappa a_i}}{\kappa} \left(a_i + \frac{1}{\kappa} \right) - \frac{e^{-\kappa b_i}}{\kappa} \left(b_i + \frac{1}{\kappa} \right) \right], \tag{9a}$$

$$\gamma_{ii} = \int_{S_i} \chi_i \, \mathrm{d}S = -\frac{1}{2} \left[\frac{1}{\kappa a_i} - \left(1 + \frac{1}{\kappa a_i} \right) e^{-2\kappa a_i} \right]. \tag{9b}$$

Substituting Eqs. (8) and (9) into Eq. (7), we obtain

$$\frac{1}{2}\Delta\psi_{S_1}=\int_{S_1}\Delta\psi_{S_1}\chi_1\,\mathrm{d}S+\int_{S_2}\psi_{S_2}\chi_2\,\mathrm{d}S+\frac{\rho_2}{\varepsilon}\beta_{22}, \tag{10a}$$

$$\frac{1}{2}\Delta\psi_{S_2}=\int_{S_2}\Delta\psi_{S_2}\chi_2\,\mathrm{d}S+\int_{S_1}\psi_{S_1}\chi_1\,\mathrm{d}S+\frac{\rho_1}{\varepsilon}\beta_{11}. \tag{10b}$$

This is an implicit expression for $\Delta\psi_{S_i}$, which has the form of an integral equation with an inseparable kernel. To obtain $\Delta\psi_{S_i}$ from Eqs. (10a) and (10b), we assume that the surface integral of a smooth function F can be approximated by

$$\int F\,\mathrm{d}S\approx\sum_{i=1}^{M}W_iF_i, \tag{11}$$

where w_i is a weighting factor, and F_i the value of F at point i. The values of w_i and M depend on the integration scheme adopted. On the basis of Eq. (11), Eqs. (10a) and (10b) can be approximated by

$$\underline{\chi}\underline{\Delta\psi}=\underline{B}, \tag{12}$$

where

$$\underline{\Delta\psi}=[\Delta\psi_{1,1},\Delta\psi_{1,2},\ldots,\Delta\psi_{1,M},\Delta\psi_{2,1},\ldots,\Delta\psi_{2,M}]^{\mathrm{t}}, \tag{12a}$$

$$\underline{\chi}=\begin{bmatrix}\underline{\chi}_{1,1} & \underline{\chi}_{1,2}\\ \underline{\chi}_{2,1} & \underline{\chi}_{2,2}\end{bmatrix}, \tag{12b}$$

$$\underline{\chi}_{l,k}=[\chi_{i,j,l,k}],\quad i,j=1,\ldots,M,\ l,k=1,2, \tag{12c}$$

$$\chi_{i,j,l,k}=\begin{cases}-w_j\chi_{k,j}^{l,i}, & i,j=1,\ldots,M, \quad l,k=1,2,\\ \dfrac{1}{2}-w_j\chi_{k,j}^{l,i}, & i=j \text{ and } l=k,\ i,j=1,\ldots,M, \quad l,k=1,2,\end{cases} \tag{12d}$$

$$\underline{B}=\begin{bmatrix}\psi_{S_2}^0\gamma_{12,1}+\dfrac{\rho_2}{\varepsilon}\beta_{12,1}\\ \vdots\\ \psi_{S_2}^0\gamma_{12,M}+\dfrac{\rho_2}{\varepsilon}\beta_{12,M}\\ \psi_{S_1}^0\gamma_{21,1}+\dfrac{\rho_1}{\varepsilon}\beta_{21,1}\\ \vdots\\ \psi_{S_1}^0\gamma_{21,M}+\dfrac{\rho_1}{\varepsilon}\beta_{21,M}\end{bmatrix}. \tag{12e}$$

In these expressions, the superscript t denotes the transpose of a matrix, $\chi_{k,j}^{l,i}$ is the value of χ in which the

Fig. 2. Variation of the scaled electrical interaction energy V_R^* between two particles as a function of $\kappa(R-a_1-a_2)$ for the case $\rho_1=\rho_2$, $a_1=a_2$, $b_1=b_2$ and $b_1/a_1=1.1$. Key: ——: exact numerical result based on Eqs. (12) and (18); ×: result based on the approximate expression, Eq. (23); △: result based on linear superposition; ○: result based on ion-penetrable (porous) model. Parameter used are: **1**: $\kappa a_1=0.02$; **2**: $\kappa a_1=0.1$; **3**: $\kappa a_1=0.8$; **4**: $\kappa a_1=1$; **5**: $\kappa a_1=10$; **6**: $\kappa a_1=15$.

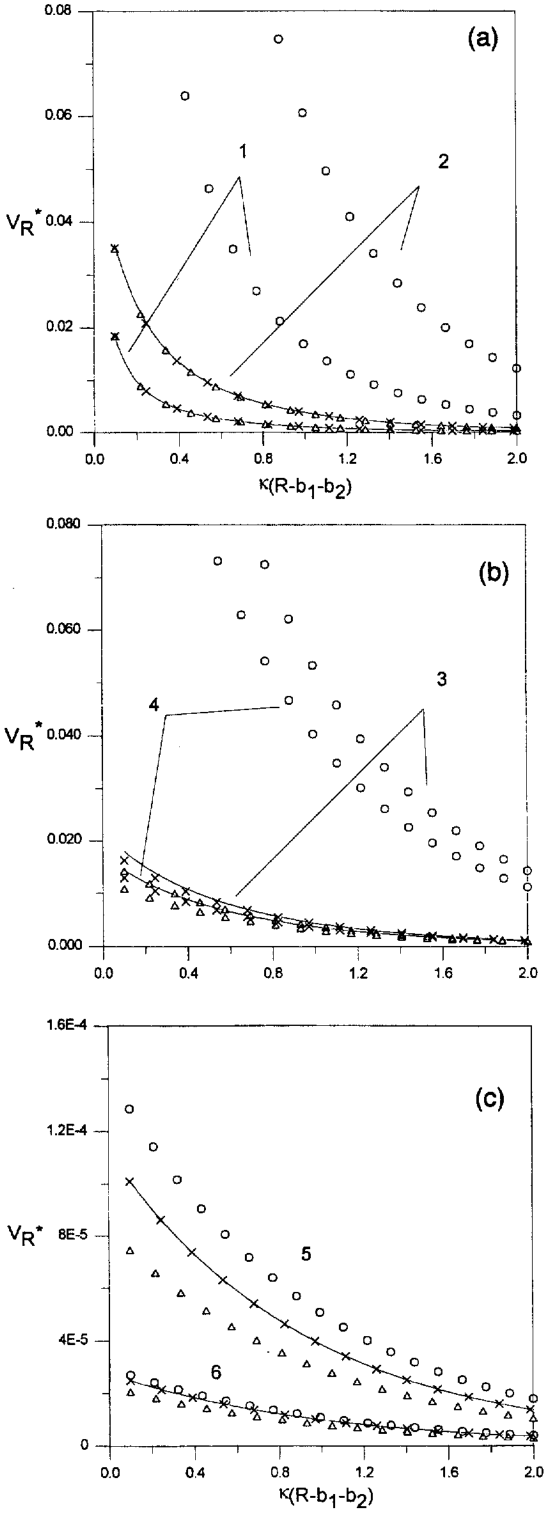

(a)
(b)
(c)
V_R^*
$\kappa(R-b_1-b_2)$
1
2
3
4
5
6
0.00
0.02
0.04
0.06
0.08
0.000
0.020
0.040
0.060
0.080
0
4E-5
8E-5
1.2E-4
1.6E-4
0.0
0.4
0.8
1.2
1.6
2.0

distance r is measured from the point j of particle k to the point i of particle l, and the differentiation in Eq. (6a) is performed on S_k, $\gamma_{ji,k}$ and $\beta_{ji,k}$ denote, respectively, the values of γ_{ji} and β_{ji} evaluated at the point k of particle j. β_{ji} and γ_{ji} are calculated by

$$\beta_{ji} = \int_{V_i} G_j \,\mathrm{d}V = \left\{ \left[b_i \cosh(\kappa b_i) - \sinh(\kappa b_i)/\kappa \right] - \left[a_i \cosh(\kappa a_i) - \sinh(\kappa a_i)/\kappa \right] \right\} \frac{\mathrm{e}^{-\kappa r_{ji}}}{\kappa^2 r_{ji}} = \zeta'_{ii} \frac{\mathrm{e}^{-\kappa r_{ji}}}{r_{ji}}, \tag{13a}$$

$$\gamma_{ji} = \int_{S_i} \chi_{ji} \,\mathrm{d}S = \frac{a_i}{2} \left[1 - \frac{1}{\kappa a_i} + \left(1 + \frac{1}{\kappa a_i} \right) \mathrm{e}^{-2\kappa a_i} \right] \mathrm{e}^{\kappa a_i} \frac{\mathrm{e}^{-\kappa r_{ji}}}{r_{ji}} = \gamma'_{ii} \frac{\mathrm{e}^{-\kappa r_{ji}}}{r_{ji}}. \tag{13b}$$

In these expressions G_j and χ_{ji} denote the target points located on S_j. Note that, if $l = k$ and $i = j$, then $\chi^{l,i}_{k,j}$ is singular. In this case, we suggest using the following approach to evaluate its value. According to Eq. (9b), $\chi^{k,j}_{k,j}$ can be evaluated by subtracting the contribution of all other $\chi^{l,i}_{k,j}$, $l \neq k$ and $i \neq j$, from γ_{kk}. We have

$$\chi_{j,j,k,k} = \frac{1}{2} - \gamma_{kk} + \sum_{\substack{i=1 \\ i \neq j}}^{M} W_i \chi^{k,j}_{k,i}. \tag{14}$$

Note that, if the fixed charges are distributed nonuniformly in the membrane phase of a particle, ρ_i is not constant, and the element $\rho_i \beta_{ji,k}$ in Eq. (12e) needs to be replaced by $\int_{V_i} \rho_i G_j \,\mathrm{d}V$.

2.1. Electrical interaction energy

For the present system, the electrical interaction energy can be estimated by

$$V_R = \frac{1}{2} \int_{V_1} \rho_1 (\psi - \psi_1^0) \,\mathrm{d}V + \frac{1}{2} \int_{V_2} \rho_2 (\psi - \psi_2^0) \,\mathrm{d}V, \tag{15}$$

where ψ_i^0 denotes the unperturbed electrical potential contributed by isolated particle i. Substituting Eqs. (6), (8) and (9) into this expression, we obtain

$$V_R = \frac{1}{2} \rho_1 \zeta_{11} \int_{S_1} \Delta \psi_{S_1} \,\mathrm{d}S + \frac{1}{2} \rho_2 \zeta_{22} \int_{S_2} \Delta \psi_{S_2} \,\mathrm{d}S + \frac{1}{2} \rho_1 \zeta'_{11} \int_{S_2} \psi_{S_2} \Theta_{21} \,\mathrm{d}S + \frac{1}{2} \rho'_2 \zeta'_{22} \int_{S_1} \psi_{S_1} \Theta_{12} \,\mathrm{d}S$$
$$+ 4\pi \zeta'_{11} \zeta'_{22} \frac{\mathrm{e}^{-\kappa r}}{R}, \tag{16}$$

where

$$\zeta_{ii} = \int_{V_i} \chi_{ii} \,\mathrm{d}V = \beta_{ii} \left[\kappa \cosh(\kappa a_i) - 1/a_i \right], \tag{16a}$$

$$\Theta_{ji} = \frac{\partial}{\partial a_j} \left(\frac{\mathrm{e}^{-\kappa r_{ji}}}{r_{ji}} \right). \tag{16b}$$

Fig. 3. Variation of the scaled electrical interaction energy V_R^* between two particles as a function of $\kappa(R - a_1 - a_2)$. The conditions are the same as those of Fig. 2 except that $b_1/a_1 = 2$.

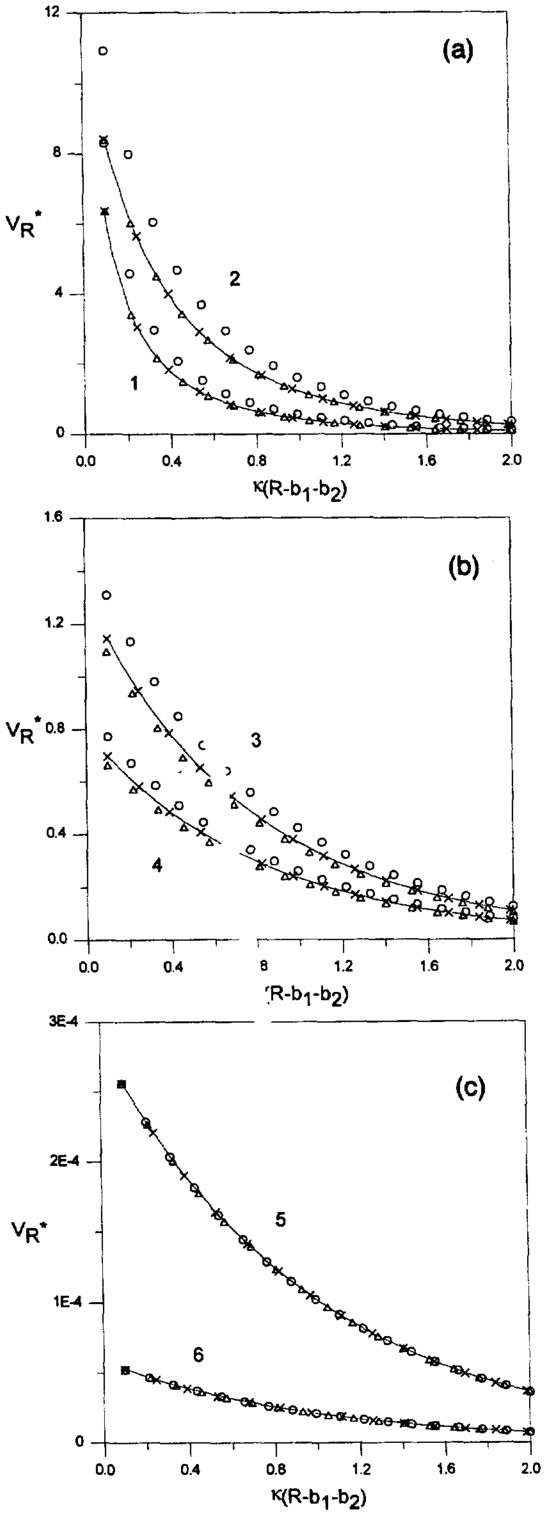
(a)
(b)
(c)
V_R^*
$\kappa(R-b_1-b_2)$
1
2
3
4
5
6

Integrating both sides of Eq. (10a) over S_2, and Eq. (10b) over S_1, we have

$$\int_{S_j} \psi_{S_j} \Theta_{ji} \, \mathrm{d}S = \frac{1/2 - \gamma_{ii}}{H_{ii}} \int_{S_i} \Delta \psi_{S_i} \, \mathrm{d}S - 4\pi \frac{\rho_j}{\varepsilon} \zeta_{jj}' \frac{\mathrm{e}^{-\kappa R}}{R}, \quad i,j = 1,2, \quad i \neq j, \tag{17}$$

where

$$H_{ii} = \frac{a_i}{\kappa} \sinh(\kappa a_1). \tag{17a}$$

Applying Eq. (17), Eq. (16) becomes

$$V_R = \frac{1}{2} \rho_1 P_{11} \int_{S_1} \Delta \psi_{S_1} \, \mathrm{d}S + \frac{1}{2} \rho_2 P_{22} \int_{S_2} \Delta \psi_{S_2} \, \mathrm{d}S, \tag{18}$$

where

$$P_{ii} = \frac{(\kappa b_i - 1)(\kappa a_i + 1)\mathrm{e}^{\kappa(b_i - a_i)} - (\kappa b_i + 1)(\kappa a_i - 1)\mathrm{e}^{\kappa(a_i - b_i)}}{2 a_i^2 \kappa^3}. \tag{18a}$$

2.2. Approximate expression

The electrical interaction energy between two particles can be estimated based on Eqs. (12) and (18). In general, a numerical scheme is necessary. Since an analytical expression for the electrical interaction energy is more readily applicable to the subsequent analysis than a numerical expression, attempt is made to derive such an expression. Here, the approach proposed by McCartney et al. [20] and Bell et al. [21] is adopted. Note that $\chi_{k,j}^{l,i}$ diverges if $l = k$ and $i = j$ (i.e., at a singular point). This suggests that the $\Delta\psi_{S_i}$ and ψ_{S_i} on the right-hand side of Eqs. (10a) and (10b) can be moved out from the integral sign, and we have

$$\frac{1}{2} \Delta \psi_{S_1} = \Delta \psi_{S_1} \gamma_{11} + \Delta \psi_{S_2} \gamma_{12} + \psi_{S_2}^0 \gamma_{12} + \frac{\rho_2}{\varepsilon} \beta_{22}, \tag{19a}$$

$$\frac{1}{2} \Delta \psi_{S_2} = \Delta \psi_{S_2} \gamma_{22} + \Delta \psi_{S_1} \gamma_{21} + \psi_{S_1}^0 \gamma_{21} + \frac{\rho_1}{\varepsilon} \beta_{11}. \tag{19b}$$

Solving these equations for $\Delta\psi_{S_1}$ and $\Delta\psi_{S_2}$ yields

$$\Delta \psi_{S_1} = \frac{\left(\psi_{S_2}^0 \gamma_{22}' + \frac{\rho_2}{\varepsilon} \zeta_{22}'\right)\left(\frac{1}{2} - \gamma_{22}\right) \frac{\mathrm{e}^{-\kappa r_{12}}}{r_{12}} + \left(\psi_{S_1}^0 \gamma_{11}' + \frac{\rho_1}{\varepsilon} \zeta_{11}'\right) \gamma_{22} \frac{\mathrm{e}^{-\kappa r_{21}}}{r_{21}} \frac{\mathrm{e}^{-\kappa r_{12}}}{r_{12}}}{\left(\frac{1}{2} - \gamma_{11}\right)\left(\frac{1}{2} - \gamma_{22}\right) - \gamma_{11}' \gamma_{22}' \frac{\mathrm{e}^{-\kappa r_{21}}}{r_{21}} \frac{\mathrm{e}^{-\kappa r_{12}}}{r_{12}}}, \tag{20a}$$

$$\Delta \psi_{S_2} = \frac{\left(\psi_{S_1}^0 \gamma_{11}' + \frac{\rho_1}{\varepsilon} \zeta_{11}'\right)\left(\frac{1}{2} - \gamma_{11}\right) \frac{\mathrm{e}^{-\kappa r_{21}}}{r_{21}} + \left(\psi_{S_2}^0 \gamma_{12}' + \frac{\rho_2}{\varepsilon} \zeta_2'\right) \gamma_{11} \frac{\mathrm{e}^{-\kappa r_{21}}}{r_{21}} \frac{\mathrm{e}^{-\kappa r_{12}}}{r_{12}}}{\left(\frac{1}{2} - \gamma_{11}\right)\left(\frac{1}{2} - \gamma_{22}\right) - \gamma_{11}' \gamma_{22}' \frac{\mathrm{e}^{-\kappa r_{21}}}{r_{21}} \frac{\mathrm{e}^{-\kappa r_{12}}}{r_{12}}}. \tag{20b}$$

Fig. 4. Variation of the scaled electrical interaction energy between two particles V_R^* as a function of $\kappa(R - a_1 - a_2)$. The conditions are the same as those of Fig. 2 except that $b_1 / a_1 = 10$.

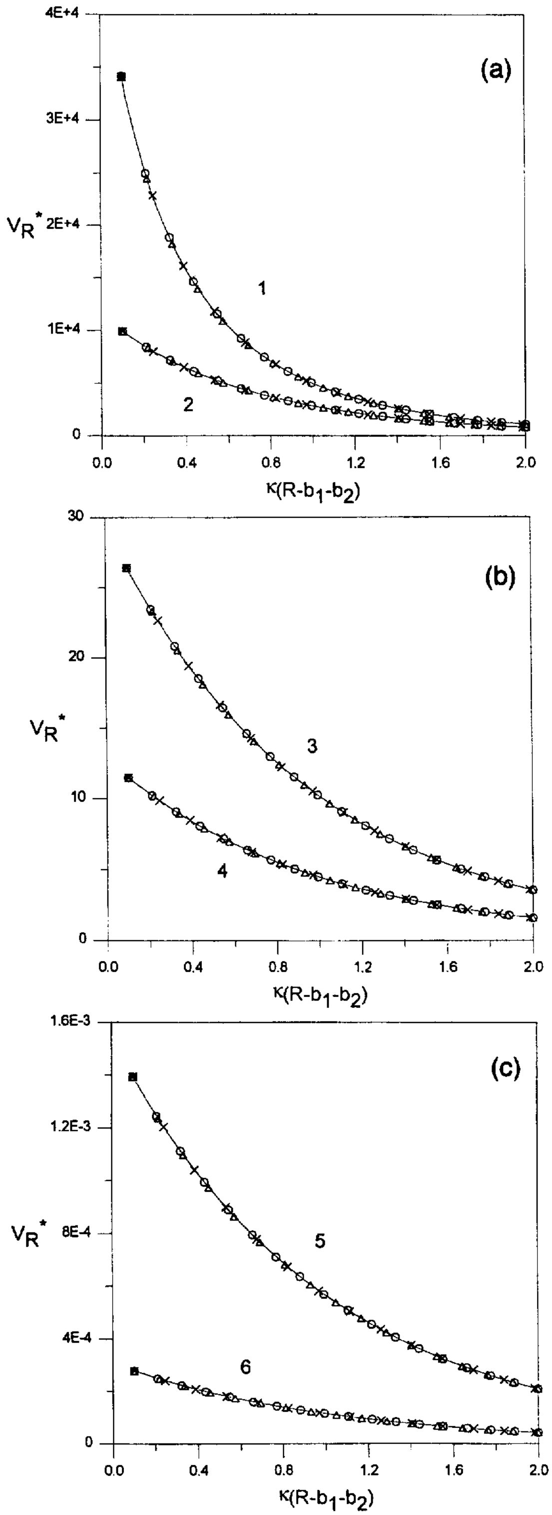
4E+4
3E+4
2E+4
1E+4
0
V_R^*
(a)
1
2
0.0
0.4
0.8
1.2
1.6
2.0
κ(R-b1-b2)
30
20
10
0
V_R^*
(b)
3
4
0.0
0.4
0.8
1.2
1.6
2.0
κ(R-b1-b2)
1.6E-3
1.2E-3
8E-4
4E-4
0
V_R^*
(c)
5
6
0.0
0.4
0.8
1.2
1.6
2.0
κ(R-b1-b2)

If the double layer is thin, we are concerned only with the points that make a small angle between r_{ji} and R. In this case, Eqs. (20a) and (20b) can be approximated by [22]

$$\Delta\psi_{S_1}=\frac{\left(\psi^0_{S_2}\gamma'_{22}+\frac{\rho_2}{\varepsilon}\zeta'_{22}\right)\left(\frac{1}{2}-\gamma_{22}\right)+\left(\psi^0_{S_1}\gamma'_{11}+\frac{\rho_1}{\varepsilon}\zeta'_{11}\right)\gamma_{22}\frac{e^{\kappa(a_2-a_1)}}{R-a_2}e^{-\kappa r_{12}}}{\left(\frac{1}{2}-\gamma_{11}\right)\left(\frac{1}{2}-\gamma_{22}\right)-\gamma'_{11}\gamma'_{22}\frac{e^{\kappa(a_2-a_1)}}{(R-a_1)(R-a_2)}e^{-2\kappa r_{12}}}\frac{e_{-\kappa r_{12}}}{r_{12}}, \tag{21a}$$

$$\Delta\psi_{S_2}=\frac{\left(\psi^0_{S_1}\gamma'_{11}+\frac{\rho_1}{\varepsilon}\zeta'_{11}\right)\left(\frac{1}{2}-\gamma_{11}\right)+\left(\psi^0_{S_2}\gamma'_{22}+\frac{\rho_2}{\varepsilon}\zeta'_{22}\right)\gamma_{11}\frac{e^{\kappa(a_1-a_2)}}{R-a_1}e^{-\kappa r_{21}}}{\left(\frac{1}{2}-\gamma_{11}\right)\left(\frac{1}{2}-\gamma_{22}\right)-\gamma'_{11}\gamma'_{22}\frac{e^{\kappa(a_1-a_2)}}{(R-a_1)(R-a_2)}e^{-2\kappa r_{21}}}\frac{e^{-\kappa r_{21}}}{r_{21}}. \tag{21b}$$

Substituting these expressions into Eq. (18), and noting that

$$\ln(1+ab)\approx b\ln(1+a),\quad a,b\to 0 \tag{22}$$

we arrive at, after some algebraic manipulations,

$$V_R=-\frac{\pi a_1a_2}{2\varepsilon f_a\kappa R}\left[\left(\tilde{\psi}_1-\tilde{\psi}_2\right)^2\ln\left(1+\sqrt{f_b}\,e^{-\kappa(R-a_1-a_2)}\right)+\left(\tilde{\psi}_1+\tilde{\psi}_2\right)^2\ln\left(1-\sqrt{f_b}\,e^{-\kappa(R-a_1-a_2)}\right)\right], \tag{23}$$

where

$$f_a=\left(\frac{1}{2}-\gamma_{11}\right)\left(\frac{1}{2}-\gamma_{22}\right), \tag{23a}$$

$$f_b=\frac{a_1a_2\left(\frac{1}{2}+\gamma_{11}\right)\left(\frac{1}{2}+\gamma_{22}\right)}{(R-a_1)(R-a_2)f_a}, \tag{23b}$$

$$\tilde{\psi}_{11}=\rho_1P_{11}a_1\sqrt{\frac{\left(\frac{1}{2}+\gamma_{22}\right)(1-e^{-2\kappa a_1})}{(\kappa a_1+1)(R-a_2)}}, \tag{23c}$$

$$\tilde{\psi}_{22}=\rho_2P_{22}a_2\sqrt{\frac{\left(\frac{1}{2}+\gamma_{11}\right)(1-e^{-2\kappa a_1})}{(\kappa a_1+1)(R-a_1)}}. \tag{23d}$$

3. Discussion

The variation of the dimensionless interaction energy, V_R^*, scaled by $\rho_1^2a_1^5/\varepsilon$, as a function of $\kappa(R-a_1-a_2)$ at various inverse Debye length κ and thickness of membrane phase are shown in Figs. 2–5. As can be seen from Figs. 2–4, for two identical particles, the approximate analytic expression, Eq. (23), is sufficiently close to

Fig. 5. Variation of the scaled electrical interaction energy between two particles V_R^* as a function of $\kappa(R-a_1-a_2)$. The conditions are the same as those of Fig. 2 except that $a_1=a_2$, $b_1=b_2$, $b_1/a_1=1.1$, and $b_2/a_2=10$.

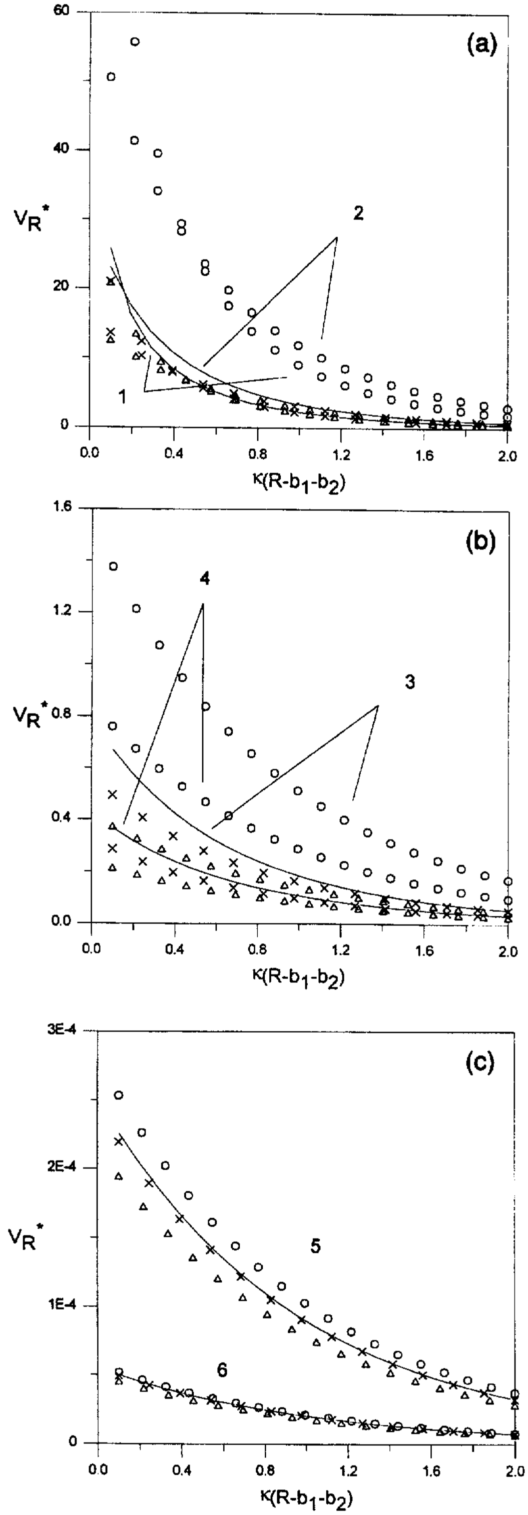
(a)
(b)
(c)
V_R^*
κ(R-b1-b2)
1
2
3
4
5
6

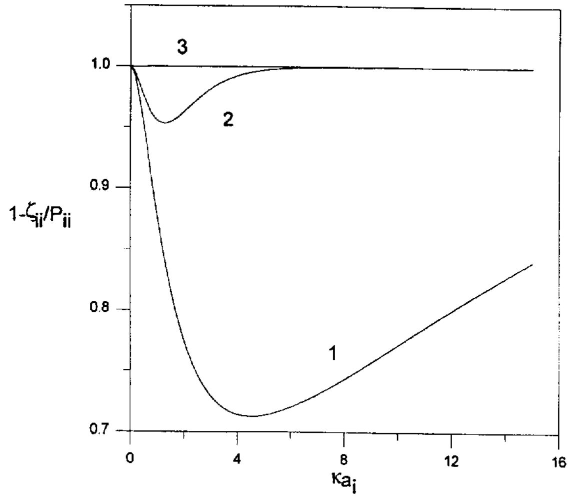

Fig. 6. Variation of $(1-\zeta_{ii}/P_{ii})$ as a function of κa_i for the case of two identical particles. Parameter used are **1**: $b_i/a_i = 1.1$; **2**: $b_i/a_i = 2$; **3**: $b_i/a_i = 10$.

the exact numerical result, which is estimated by substituting Eq. (12) into Eq. (18). As suggested by Fig. 5, the performance of Eq. (23) becomes less satisfactory for two different particles, especially when the double layer is thick (small κa_1). Figs. 2–5 reveal that the performance of Eq. (23) is satisfactory if the double layer is either very thin or very thick, it is less satisfactory for an intermediate thickness of double layer.

Note that if the double layer is very thin, Eq. (23) may lead to an appreciable deviation due to the limitation of the precision of a computing facility. This can be alleviated by applying the approximate relation $\ln(1+x) \approx x$ to Eq. (23), and we obtain

$$V_R = 4\pi \frac{\rho_1 \rho_2}{\varepsilon} \frac{a_1^2 a_2^2 P_{11} P_{22}}{(\kappa a_1 + 1)(\kappa a_2 + 1)} \frac{e^{-(R-a_1-a_2)}}{R} \equiv V_R^{\mathrm{app}}. \tag{24}$$

This expression can also be obtained by neglecting the second term on the right-hand side of both Eqs. (19a) and (19b), and substituting the resultant expressions into Eq. (18).

3.1. Linear superposition

Linear superposition is one of the idealized procedures often adopted in the literature for a system which involves more than one charged entities. In this approach, the desired property of each isolated entities is evaluated, and then summed over all the entities by choosing an adequately defined global coordinate. The result thus obtained is used to approximate the property of the whole system. Adopting this approach, Eq. (15) becomes

$$V_R = \frac{1}{2}\int_{V_1} \rho_1 \psi_2^0 \, dV + \frac{1}{2}\int_{V_2} \rho_2 \psi_1^0 \, dV. \tag{25}$$

Substituting Eqs. (6) and (9) into this expression yields

$$V_R = 2\pi \frac{\rho_1 \rho_2}{\varepsilon} \left(\zeta'_{11} P_{22} \frac{a_2^2 e^{\kappa a_2}}{\kappa a_2 + 1} + \zeta'_{22} P_{11} \frac{a_1^2 e^{\kappa a_1}}{\kappa a_1 + 1} \right) \frac{e^{-\kappa R}}{R}. \tag{26}$$

The scaled electrical interaction energy between two particles based on this expression is also shown in Figs. 2–5 for comparison. These figures reveal that linear superposition will underestimate the interaction energy, in general. However, its performance can be satisfactory if the double layer is either very thin or very thick, or the membrane phase is thick. This can be explained as below. Let us consider the case of an isolated particle the core of which is ion-penetrable and contains fixed charges such that Eq. (5) is satisfied. Then the electrical potential distribution outside the core of this particle is the same as that of a particle with a rigid core. For two particles both have an ion-penetrable core, if the double layer is very thick (κ very small), the induced net charges in the rigid core of a particle due to the application of linear superposition is limited. In this case, although Eq. (5) is no longer satisfied exactly, the deviation can be adjusted by adding some positive and negative charges to the ion-penetrable core of a particle. This has but an insignificant influence on the interaction energy between two particles. On the other hand, if the double layer is very thin (κ very large), its influence on the charged condition of the rigid core of a particle is negligible, and the linear superposition becomes appropriate. The effect of the thickness of membrane phase on the performance of linear superposition will be elaborated latter.

Eq. (26) can be rewritten as

$$V_R = V_R^{\mathrm{app}}\left[\frac{(1-\zeta_{11}/P_{11})+(1-\zeta_{22}/P_{22})}{2}\right]. \tag{27}$$

This expression reveals that the closer the $(1-\zeta_{ii}/P_{ii})$ to unity, the closer the performance of the linear superposition to the approximate solution, Eq. (24). As can be seen from Fig. 6, this is the case when the membrane phase is thick, or the double layer is either very thin or very thick. In other words, the linear superposition is appropriate for these cases.

3.2. Entirely ion-penetrable particles

The problem of two entirely ion-penetrable (porous) particles is one of the special cases of the present analysis. In this case, the electrical interaction energy based on Eq. (25) becomes exact, and it can be shown that

$$V_R = 4\pi\frac{\rho_1\rho_2}{\varepsilon}\zeta'_{11}(a_1=0)\zeta'_{22}(a_2=0)\frac{e^{-\kappa R}}{R}. \tag{28}$$

This is consistent with the result of Ohshima et al. [12].

For comparison, the results for the case of entirely ion-penetrable particles are also illustrated in Figs. 2–5. As can be seen from these figures, for the same ρ_i, entirely ion-penetrable particles have a higher electrical interaction energy than particles comprises a rigid core and a membrane layer, as expected. However, if the membrane layer is thick and/or the double layer is thin, the two cases lead to about the same electrical interaction energy. This is because that if the membrane layer is thick and/or the double layer is thin, the Donnan potential is reached [23] at some point P inside the membrane layer. This implies that there are no net charges in the region between the center of a particle and P, and the region behaves like a rigid core. It is also possible to simulate a particle with a thin membrane layer by a particle that has the same thickness of membrane but with an uncharged, ion-penetrable core, that is, an ion-penetrable membrane shell. This is because that in this case the $\zeta'_{ii}(a_i=0)$ in Eq. (28) should be replaced by ζ'_{ii}, and we have

$$V_R = V_R^{\mathrm{app}}(1-\zeta_{11}/P_{11})(1-\zeta_{22}/P_{22}). \tag{29}$$

According to the conclusion drawn from Fig. 6, the performance of this expression can be satisfactory under the condition that the linear superposition is appropriate.

Acknowledgements

This work is supported by the National Science Council of the Republic of China.

References

[1] R.J. Hunter, Foundations of Colloid Science, vol. 1, Oxford University Press, London, 1989.
[2] E.J.W. Verwey, J.Th.G. Overbeek, Theory of the Stability of Lyophobic Colloids, Elsevier, Amsterdam, 1948.
[3] R.W. Wunderlich, J. Colloid Interface Sci. 88 (1982) 385.
[4] S. Levine, M. Levine, K.A. Sharp, D.E. Brooks, Biophys. J. 42 (1983) 127.
[5] K.A. Sharp, D.E. Brooks, Biophys. J. 47 (1985) 563.
[6] H. Reiss, I.C. Bassignana, J. Membrane Sci. 11 (1982) 219.
[7] C. Selvey, H. Reiss, J. Membrane Sci. 23 (1985) 11.
[8] J.P. Hsu, D.P. Lin, S.J. Tseng, Colloid Polymer Sci. 273 (1995) 271.
[9] G.V. Seaman, in: D.M. Sergenor (Ed.), The Red Blood Cells, vol. 2, Academic Press, New York, 1975.
[10] H. Ohshima, K. Makino, T. Kondo, J. Colloid Interface Sci. 113 (1986) 369.
[11] H. Ohshima, T. Kondo, J. Theor. Biol. 128 (1987) 187.
[12] H. Ohshima, T. Kondo, J. Colloid Interface Sci. 155 (1993) 499.
[13] J.P. Hsu, W.C. Hsu, Y.I. Chang, J. Colloid Interface Sci. 165 (1994) 1.
[14] J.P. Hsu, W.C. Hsu, Y.I. Chang, J. Colloid Interface Sci. 160 (1993) 505.
[15] J.P. Hsu, Y.C. Kuo, J. Colloid Interface Sci. 171 (1995) 483.
[16] J.P. Hsu, Y.C. Kuo, J. Chem. Phys. 103 (1995) 465.
[17] S.L. Carnie, D.Y.C. Chan, J. Stankovich, J. Colloid Interface Sci. 165 (1994) 116.
[18] M.D. Greenberg, Application of Green's Functions in Science and Engineering, Prentice-Hall, Englewood Cliffs, NJ, 1971.
[19] H. Jeffreys, B.S. Jeffreys, Methods of Mathematical Physics, Cambridge University Press, Cambridge, 1956.
[20] L.N. McCartney, S. Levine, J. Colloid Interface Sci. 30 (1969) 345.
[21] G.M. Bell, S. Levine, L.N. McCartney, J. Colloid Interface Sci. 33 (1970) 335.
[22] J.E. Sader, S.L. Carnie, D.Y.C. Chan, J. Colloid Interface Sci. 171 (1995) 46.
[23] H. Ohshima, T. Kondo, J. Theor. Biol. 124 (1987) 191.